Inorganica Chimica Acta 363 (2010) 294–300

Contents lists available at ScienceDirect

Inorganica Chimica Acta

journal homepage: www.elsevier.com/locate/ica

^{1}H NMR spectroscopy as a tool to determine accurate photoisomerization quantum yields of stilbene-like ligands coordinated to rhenium(I) polypyridyl complexes

Karina Passalacqua Morelli Frin, Melina Kayoko Itokazu, Neyde Yukie Murakami Iha *

Laboratory of Photochemistry and Energy Conversion, Instituto de Química, Universidade de São Paulo – USP, Av. Prof. Lineu Prestes, 748, 05508-900 São Paulo, SP, Brazil

ARTICLE INFO

Article history:
Received 13 August 2009
Accepted 14 October 2009
Available online 20 October 2009

Keywords:
^{1}H NMR spectroscopy
True quantum yield
Rhenium(I) complexes
Trans to *cis* photoisomerization
Stilbene-like ligands

ABSTRACT

In this work, the use of proton nuclear magnetic resonance, ^{1}H NMR, was fully described as a powerful tool to follow a photoreaction and to determine accurate quantum yields, so called true quantum yields (Φ_{true}), when a reactant and photoproduct absorption overlap. For this, Φ_{true} for the *trans–cis* photoisomerization process were determined for rhenium(I) polypyridyl complexes, *fac*-[Re(CO)$_3$(NN)(*trans*-L)]$^+$ (NN = 1,10-phenanthroline, phen, or 4,7-diphenyl-1,10-phenanthroline, ph$_2$phen, and L = 1,2-bis(4-pyridyl)ethylene, bpe, or 4-styrylpyridine, stpy). The true values determined at 365 nm irradiation (e.g. Φ_{NMR} = 0.80 for *fac*-[Re(CO)$_3$(phen)(*trans*-bpe)]$^+$) were much higher than those determined by absorption spectral changes (Φ_{UV-Vis} = 0.39 for *fac*-[Re(CO)$_3$(phen)(*trans*-bpe)]$^+$). Φ_{NMR} are more accurate in these cases due to the distinct proton signals of *trans* and *cis*-isomers, which allow the actual determination of each component concentration under given irradiation time. Nevertheless when the photoproduct or reactant contribution at the probe wavelength is negligible, one can determine Φ_{true} by regular absorption spectral changes. For instance, $\Phi_{313\ nm}$ for free ligand photoisomerization determined both by absorption and ^{1}H NMR variation are equal within the experimental error (bpe: Φ_{UV-Vis} = 0.27, Φ_{NMR} = 0.26; stpy: Φ_{UV-Vis} = 0.49, Φ_{NMR} = 0.49). Moreover, ^{1}H NMR data combined with electronic spectra allowed molar absorptivity determination of difficult to isolate *cis*-complexes.

1. Introduction

The *trans* to *cis* photoisomerization reaction of *trans* stilbene-like compounds (*trans*-L) has been extensively investigated. Although the mechanisms are still under investigation, it has been reported that both singlet and triplet pathways are involved in the photoisomerization process [1–8]. When *trans*-1,2-bis(4-pyridyl)ethylene (bpe) is coordinated to a heavy atom, such as rhenium(I) in *fac*-[Re(CO)$_3$(phen)(*trans*-bpe)]$^+$, the coupling between the singlet and triplet manifolds is enhanced [9]. The complex acts as a sensitizer through an energy transfer from the ^{3}MLCT excited state to the ^{3}IL one, which is the only pathway to reach the excited state responsible for the isomerization. On the other hand, for the coordinated *trans*-4-styrylpyridine (stpy), a contribution of the singlet pathway is also considered in the photoisomerization process [10].

Another interesting feature of the *trans* to *cis* photoisomerization of stilbene-like ligands coordinated to *fac*-[Re(CO)$_3$(NN)(*trans*-L)]$^+$ (NN = polypyridyl ligands) is their sensitization to visible region, which can be an advantage over their free organic counterparts, and more suitable to be exploited in the development of molecular devices.

The photoinduced isomerization quantum yields for the coordinated *trans*-L to rhenium(I) complexes have been usually determined by the variation of absorbance [10–21]. However, when both the reactant and photoproduct absorb in the same spectral region, quantum yields obtained by absorption spectral changes are only apparent. Therefore, another technique is required to follow the *trans* to *cis* photoisomerization reaction and to determine true quantum yields. The best approach in these cases is the proton nuclear resonance spectroscopy, ^{1}H NMR, since both the chemical shifts and coupling constants, especially for the olefinic protons, are fairly different for the two isomers. Previously, this technique has only been employed to demonstrate the occurrence of the photoisomerization processes in these complexes [13,15,22], although it can provide accurate quantum yields for the isomerization process of coordinated *trans*-L ligands. Moreover, the use of NMR spectroscopy is not limited to follow only photoreactions; this technique is as good for any reaction kinetics wherein a product and a reactant absorb in the same spectral region.

In this work, the use of proton nuclear magnetic resonance, ^{1}H NMR, is fully described and showed as a powerful tool to follow the photoprocess and to determine accurate photoisomerization

* Corresponding author: Tel.: +55 11 3091 2151; fax: +55 11 3915 5571.
E-mail address: neydeiha@iq.usp.br (N.Y. Murakami Iha).

0020-1693/$ - see front matter © 2009 Elsevier B.V. All rights reserved.
doi:10.1016/j.ica.2009.10.008

quantum yields. Moreover, the molar absorptivities of difficult to isolate photoproducts can be obtained by association of ^{1}H NMR and absorption variation measurements. Therefore, the true quantum yields can be determined without the use of further NMR experiments. This approach has been exploited by determining true quantum yields for the *fac*-[Re(CO)$_3$(NN)(*trans*-L)]$^+$ complexes (NN = 1,10-phenanthroline, phen, or 4,7-diphenyl-1,10-phenanthroline, ph$_2$phen, and L = 1,2-bis(4-pyridyl)ethylene, bpe, or 4-styrylpyridine, stpy) and were compared with the ones determined only by absorption variations.

2. Experimental

2.1. Materials

All chemicals, Aldrich, were reagent grade, except deuterated grade solvent, Aldrich or Cambridge, for photochemical measurements. [ClRe(CO)$_5$], Strem, 1,10-phenanthroline (phen), QM, and 4,7-diphenyl-1,10-phenanthroline (ph$_2$phen), trifluoromethanesulfonic acid (tfms) and *trans*-1,2-bis(4-pyridyl)ethylene (*trans*-bpe), Aldrich, were used as received. Potassium tris(oxalate) ferrate(III) was prepared and purified according to the literature procedure [23]. *trans*-4-styrylpyridine (*trans*-stpy) was prepared as previously reported [18]. ^{1}H NMR (CD$_3$CN, δ/ppm): 8.53 (d, 2H); 7.62 (d, 2H); 7.47 (d, 2H); 7.41 (d, 1H); 7.41 (t, 2H); 7.34 (t, 1H); 7.17 (d, 1H).

2.2. Syntheses of rhenium(I) complexes

fac-[ClRe(CO)$_3$(NN)] complexes (NN = phen or ph$_2$phen) were prepared according to the literature procedure [17,18,20,24]. [ClRe(CO)$_5$] and an excess of the NN ligand were suspended in xylene and heated to reflux for several hours. The crude product was recrystallized from dichloromethane by slow addition of *n*-pentane. These *fac*-[ClRe(CO)$_3$(NN)] complexes were converted to *fac*-[(tfms)Re(CO)$_3$(NN)] as previously described [17,18,20] by adding trifluoromethanesulfonic acid to *fac*-[ClRe(CO)$_3$(NN)] suspended in dichloromethane and precipitated by addition of diethyl ether.

fac-[Re(CO)$_3$(NN)(*trans*-L)]$^+$ complexes were synthesized following the procedure previously described [18,20,25] by refluxing *fac*-[(tfms)Re(CO)$_3$(NN)] with an excess of *trans*-L in methanol and precipitated with NH_4PF_6.

2.3. Methods

Electronic absorption spectra were recorded on a Hewlett Packard 8453 spectrophotometer with quartz cuvets of 1.000 or 0.100 cm optical length.

^{1}H NMR spectra were recorded on a Bruker AC-200 (200 MHz), a DPX-300 (300 MHz) or a DRX-500 (500 MHz) spectrometers at 298 K using CD$_3$CN as a solvent. The signals of residual CH$_3$CN were used as an internal standard.

The photolysis system (Oriel) has been described in detail elsewhere [17,20]. Light intensities for each irradiation wavelength were determined by actinometry using tris(oxalate)ferrate(III) before and after each photolysis experiment [26].

All irradiations were carried out in a system especially designed for this purpose with a 1.000 cm optical length quartz cuvet (photolysis compartment) directly connected to another one (0.100 cm), where absorption changes were measured. The concentration of complexes was adjusted to yield absorbances around 2 at the irradiation wavelength in the 1.000 cm cuvet. The ^{1}H NMR spectrum was registered after each photolysis time and changes in both chemical shift and coupling constant were monitored.

True quantum yields (average of at least two independent experiments at each irradiation wavelength) were determined based on the area of photoproduct and reactant proton signals. Apparent photoisomerization quantum yields (average of at least three independent experiments at each irradiation wavelength) were determined by using variation in absorption spectra (following the absorption decay in the 320–340 nm region, where the contribution of *cis*-complexes was considered as low as possible) as reported elsewhere [10,16–20].

Molar absorptivities of *fac*-[Re(CO)$_3$(NN)(*cis*-L)]$^+$ complexes were obtained by photolysis of a corresponding *trans*-isomer complex in CD$_3$CN of appropriate concentration (ca. 10^{-4} mol L^{-1}). Photolysis percentages and, consequently, concentrations of the *trans* and *cis* species were determined using the absorption spectra and ^{1}H NMR spectroscopy.

3. Results and discussion

^{1}H NMR spectral changes observed at 365 nm irradiation of *fac*-[Re(CO)$_3$(ph$_2$phen)(*trans*-bpe)]$^+$ are shown in Fig. 1. Irradiation of *trans*-isomer complexes, *fac*-[Re(CO)$_3$(NN)(*trans*-L)]$^+$, results in decrease of *trans*-isomer proton signals while the *cis*-isomer signals build up in intensity due to the isomerization process of the coordinated stilbene-like ligands, Eq. (1).

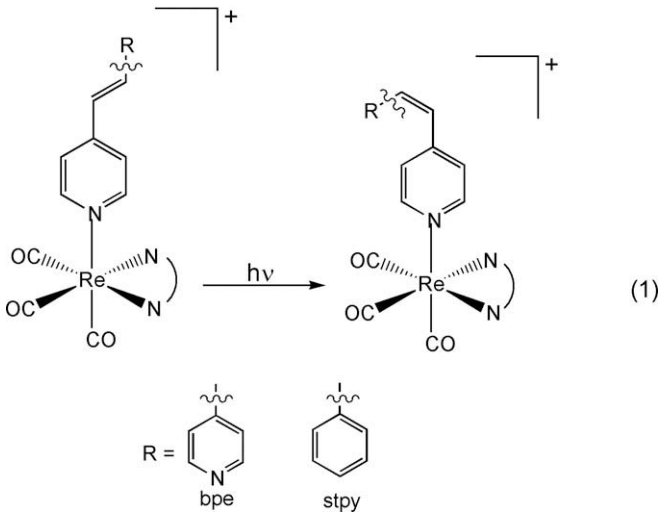

(1)

Proton signals in the 7.4–7.0 ppm region correspond to the olefinic ones (Hc and Hc′) on a *trans* configuration and display a characteristic coupling constant of 16 Hz. Under 313, 365 or 404 nm irradiation, new peaks are clearly observed as a result of the photoprocess. Shifts of the *cis*-isomer signals to lower frequencies and the coupling constant decrease of olefinic protons (Hc* and Hc′*) from 16 to 12 Hz are the main differences observed for the *fac*-[Re(CO)$_3$(ph$_2$phen)(*trans*-bpe)]$^+$ complex in comparison with the *fac*-[Re(CO)$_3$(ph$_2$phen)(*cis*-bpe)]$^+$ one.

The *fac*-[Re(CO)$_3$(NN)(*cis*-L)]$^+$ (NN = phen or ph$_2$phen and L = bpe or stpy) proton signals, although without having isolated products, are now assigned, Table 1, and are presented along with the data for the *trans*-isomer complexes [17–20] for comparison.

In this work, the photoprocess was monitored using the highest signals for each isomer, Hα′ and Hα′* (9.65–9.55 ppm region), to obtain the most accurate values, although any *cis*–*trans* proton signal pair can be used. True quantum yields, Φ_{true}, determined based on the ^{1}H NMR spectral changes were obtained by the proton signal area of *cis*-isomer and by using the Eq. (2), where n_R is the number of initial reactant, $\int P$ and $\int R$ are the area of the photoproduct and reactant signals, respectively, I_0 is the incident light intensity and t_{irr} is the irradiation time:

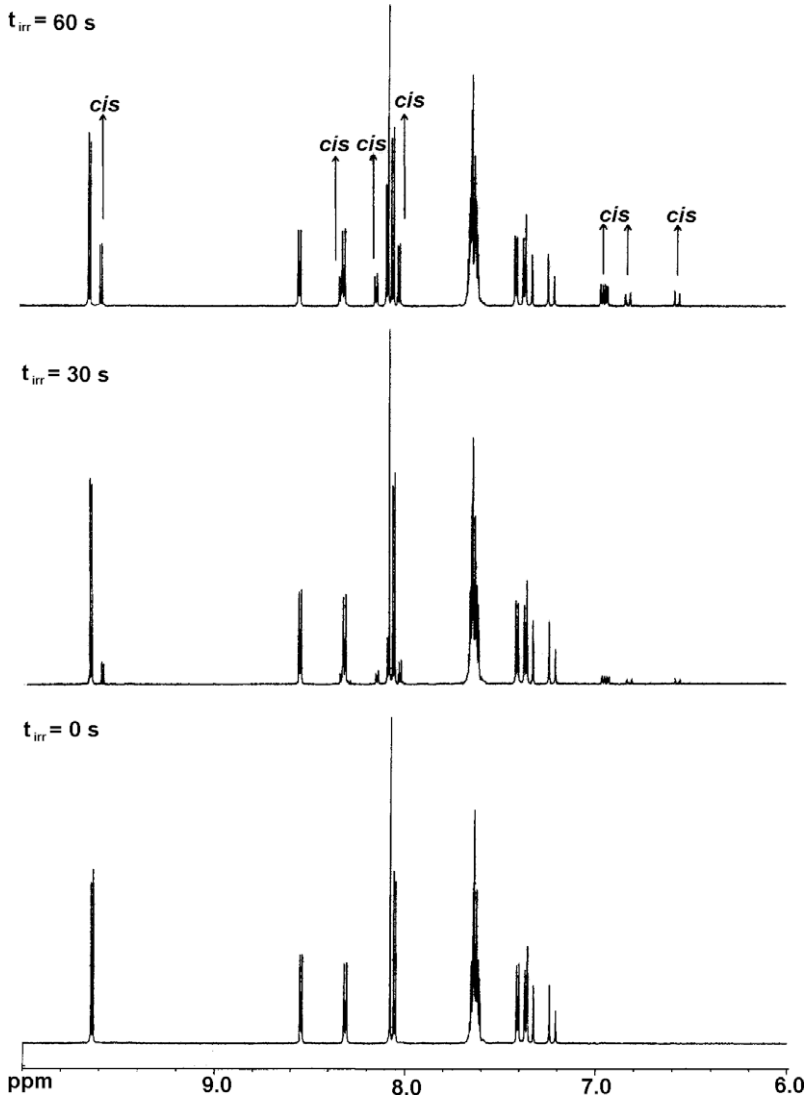

Fig. 1. ^{1}H NMR spectra of *fac*-[Re(CO)$_3$(ph$_2$phen)(*trans*-bpe)]$^+$ in CD$_3$CN upon photolysis at 365 nm. (500 MHz, 3.5×10^{-4} mol L^{-1}, T = 298 K).

$$\Phi_{\text{true}} = \frac{n_R \cdot \int P}{I_0 t_{\text{irr}} (\int R + \int P)} \tag{2}$$

Spectral changes during *trans* to *cis* photoisomerization, Fig. 2, show a decrease of the *trans* complex contribution in 270–400 nm and the appearance of the *cis* photoproduct (200–270 nm), but there is no region to monitor the contribution of each isomer itself (see inset Fig. 2). Therefore, even measuring at three different wavelengths, selected where the absorption of the *cis*-isomer is as low as possible (320–340 nm), quantum yields so determined are still apparent, Φ_{app}.

Quantum yields determined by ^{1}H NMR, Φ_{true}, are much higher than the values determined by absorption changes, Φ_{app}, Table 2, for *fac*-[Re(CO)$_3$(NN)(*trans*-L)]$^+$ in CD$_3$CN, under 313, 365 or 404 nm irradiation.

One can observe that ^{1}H NMR measurements give more accurate quantum yields, which can be considered the true ones since the *trans* and *cis*-isomers proton signals appear in fairly different frequencies. Thus, the use of ^{1}H NMR spectroscopy has been successfully employed to determine the *trans* to *cis* photoisomerization quantum yields of coordinated stilbene-like ligands. Additionally, this technique, when combined with absorption spectroscopy, allows the determination of molar absorptivities of *fac*-[Re(CO)$_3$(NN)(*cis*-L)]$^+$ complexes, $\varepsilon_{\text{cis}}(\lambda)$, in all spectral region, Fig. 3, by using Eq. (3) and *trans* and *cis*-isomer concentrations obtained by ^{1}H NMR data:

$$\varepsilon_{cis}(\lambda) = \frac{A - \varepsilon_{trans}(\lambda) \cdot b \cdot C_{trans}}{C_{cis} \cdot b} \tag{3}$$

A = absorbance of irradiated solution;
$\varepsilon_{trans}(\lambda)$ = *trans*-isomer molar absorptivities;
b = optical length;
C_{trans} = molar concentration of the *trans*-isomer;
C_{cis} = molar concentration of the *cis*-isomer.

Once molar absorptivities of *cis*-complex isomers are obtained, the molar concentration of *cis*-isomer in the irradiated solution can be determined by Eq. (3) and the number of the *cis* photoproduct, n_{cis}, is obtained by Eq. (4):

$$n_{cis} = C_{cis} \cdot V \cdot 6.023 \times 10^{23} \tag{4}$$

C_{cis} = molar concentration of the *cis*-isomer;
V = irradiated volume (L).

Therefore, each isomer contribution in absorption spectra during photolysis is determined and, consequently, the true quantum

Table 1
^{1}H NMR spectral data for *fac*-[Re(CO)$_3$(NN)(*cis*-L)]$^+$ and *fac*-[Re(CO)$_3$(NN)(*trans*-L)]$^+$ in CD_3CN (500 MHz).

Compounds	Proton	δ (ppm)	J (Hz)	Remarks
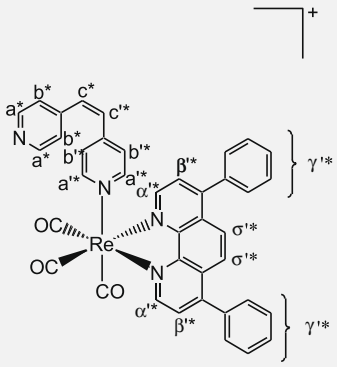	Hα′* (d, 2H)	9.58	5.3	
	Hβ′* (d, 2H)	8.02	5.3	
	Hγ′* (m, 10H)	8.09		
	Hσ′* (s, 2H)	7.63		
	Ha* (d, 2H)	8.33	6.8	
	Hb* (d, 2H)	6.96	6.8	
	Hc* (d, 1H)	6.82	**12**	
	Ha′* (d, 2H)	8.14	5.5	
	Hb′* (d, 2H)	6.94	5.5	
	Hc′* (d, 1H)	6.57	**12**	
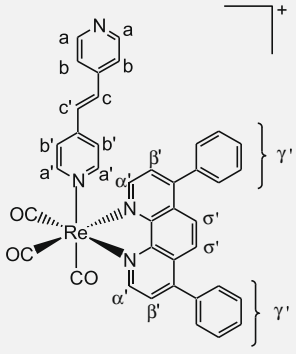	Hα′ (d, 2H)	9.64	5.4	[19,20]
	Hβ′ (d, 2H)	8.06	5.4	
	Hγ′ (m, 10H)	7.63		
	Hσ′ (s, 2H)	8.08		
	Ha (d, 2H)	8.55	6.3	
	Hb (d, 2H)	7.40	6.3	
	Hc (d, 1H)	7.34	**16**	
	Ha′ (d, 2H)	8.31	6.7	
	Hb′ (d, 2H)	7.36	6.7	
	Hc′ (d, 1H)	7.23	**16**	
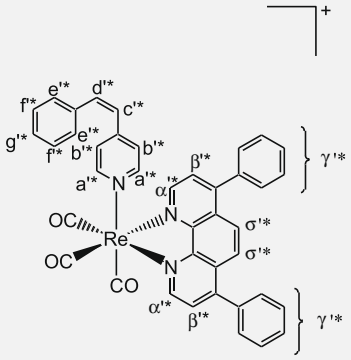	Hα′* (d, 2H)	9.59	5.4	
	Hβ′* (d, 2H)	8.04	5.4	
	Hσ′* (s, 2H)	8.09		
	Hδ′* (m, 10H)	7.65		
	Ha′* (d, 2H)	8.13	1.4; 5.4;	
	Hb′* (d, 2H)	6.99		
	Hc′* (d, 1H)	6.39	**12**	
	Hd′* (d, 1H)	6.89	**12**	
	He′* (dd, 2H)	7.05		
	Hf′* (dd, 2H)	7.18		
	Hg′* (dd, 1H)	7.25		
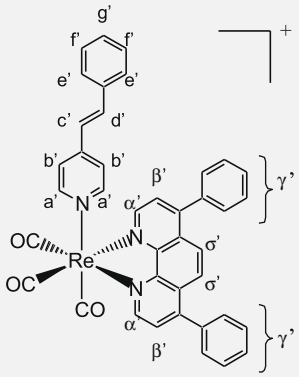	Hα′ (d, 2H)	9.64	5.4	[19]
	Hβ′ (d, 2H)	8.06	5.4	
	Hσ′ (s, 2H)	8.08		
	Hδ′ (m, 10H)	7.64		
	Ha′ (d, 2H)	8.26	6.8	
	Hc′ (d, 1H)	7.02	**16**	
	Hd′ (d, 1H)	7.41	**16**	
	He′ (dd, 2H)	7.54	1.7; 7.8	
	Hb′, Hf′, Hg′ (m, 5H)	7.36		

(*continued on next page*)

Table 1 (*continued*)

Compounds	Proton	δ (ppm)	J (Hz)	Remarks
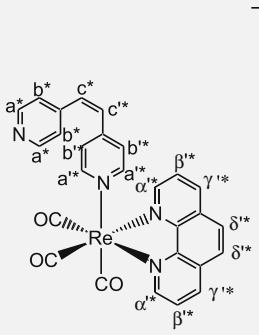	Hα′* (dd, 2H)	9.55	1.4; 5.1	
	Hβ′* (dd, 2H)	8.08	5.1; 8.3	
	Hγ′* (dd, 2H)	8.83	8.3	
	Hδ′* (s, 2H)	8.17		
	Ha* (dd, 2H)	8.25		
	Hb*, Hb′* (m, 4H)	6.88		
	Hc* (dd, 1H)	6.79	**12**	
	Ha′* (dd, 2H)	8.05	5.3; 1.6	
	Hc′* (dd, 1H)	6.52	**12**	
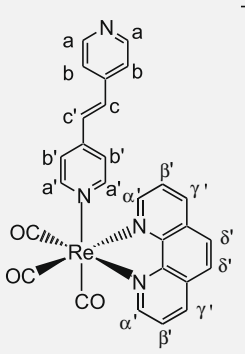	Hα′ (dd, 2H)	9.62	1.3; 5.2	[17,19]
	Hβ′ (dd, 2H)	8.12	5.2; 8.3	
	Hγ′ (dd, 2H)	8.84	1.3; 8.3	
	Hδ′ (s, 2H)	8.17		
	Ha (dd, 2H)	8.54	4.6	
	Hb (dd, 2H)	7.39	4.6	
	Hc (dd, 1H)	7.30	**16**	
	Ha′ (dd, 2H)	8.22	5.4	
	Hb′ (dd, 2H)	7.30	4.0	
	Hc′ (dd, 1H)	7.18	**16**	
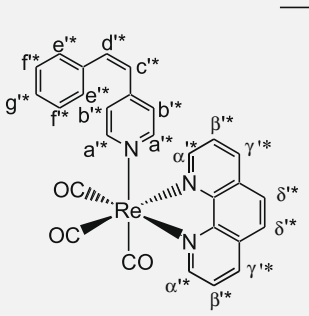	Hα′* (dd, 2H)	9.56	1.5; 5.0	
	Hβ′* (dd, 2H)	8.08	5.0; 8.3	
	Hγ′* (dd, 2H)	8.83	1.5; 4.0	
	Hδ′* (s, 2H)	8.17		
	Ha′* (dd, 2H)	8.02	1.5; 5.0	
	Hb′* (dd, 2H)	6.91	1.5; 5.0	
	Hc′* (d, 1H)	6.35	**12**	
	Hd′* (d, 1H)	6.87	**12**	
	He′* (m, 2H)	7.16		
	Hf′* (m, 2H)	6.98		
	Hg′* (m, 1H)	7.25		
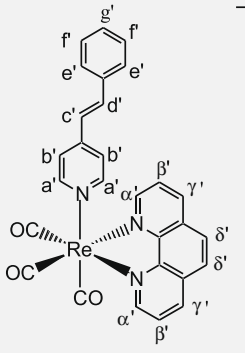	Hα′ (dd, 2H)	9.62	1.5; 5.0	[18,19]
	Hβ′ (dd, 2H)	8.12	5.0; 8.4	
	Hγ′ (dd, 2H)	8.17	1.5; 8.4	
	Hδ′ (s, 2H)	8.84		
	Ha′ (d, 2H)	8.16	5.5	
	Hb′ (d, 2H)	7.26	7.0	
	Hc′ (d, 1H)	6.97	**16**	
	Hd′ (d, 1H)	7.37	**16**	
	He′ (dd, 2H)	7.52	1.5; 8.0	
	Hf′, Hg (m, 3H)	7.35		

yields can be obtained. Thus, when the ^{1}H NMR spectroscopy is properly employed along with absorption spectrum variation, the apparent quantum yields once obtained by absorption changes can be corrected to the true values without further NMR experiments. For instance, the true quantum yields for *fac*-[Re(CO)$_3$(phen)(*trans*-bpe)]$^+$ under 404 nm irradiation and for *fac*-[Re(CO)$_3$(phen)(*trans*-stpy)]$^+$ under 313 nm irradiation, Table 2, were determined using this correction for apparent quantum yields, Φ_{app}, previously reported [10,18].

In the region employed for the quantum yield determination (320–340 nm), molar absorptivities of *fac*-[Re(CO)$_3$(ph$_2$phen)(*cis*-bpe)]$^+$ are lower than for *trans*-isomer complexes but the contribution of *cis*-complex are in the same order of magnitude (10^4 L mol^{-1} cm^{-1}) and can not be neglected. Consequently, the

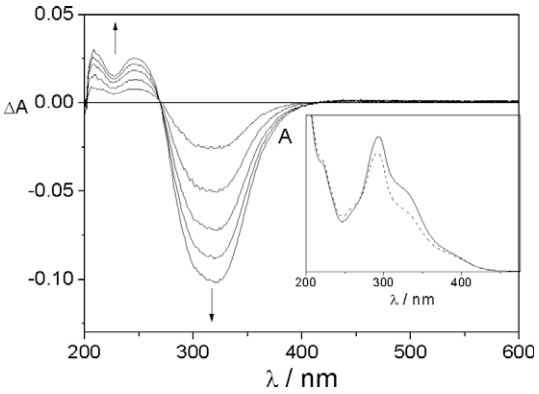

Fig. 2. Difference absorption spectra of *fac*-[Re(CO)$_3$(ph$_2$phen)(*trans*-bpe)]$^+$ in CH_3CN (3.5×10^{-4} mol L^{-1}, $\Delta t = 4$ s, $\lambda_{irr} = 365$ nm). Inset: absorption spectra of *fac*-[Re(CO)$_3$(ph$_2$phen)(*trans*-bpe)]$^+$ (——) and of a solution having 25% of *fac*-[Re(CO)$_3$(ph$_2$phen)(*cis*-bpe)]$^+$ (- - -).

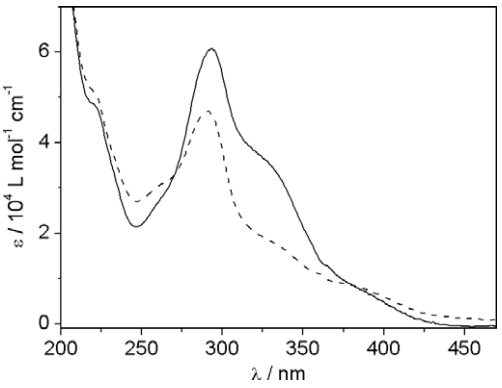

Fig. 3. Molar absorptivities of *fac*-[Re(CO)$_3$(ph$_2$phen)(*cis*-bpe)]$^+$ (- - -) in comparison with *fac*-[Re(CO)$_3$(ph$_2$phen)(*trans*-bpe)]$^+$ (——).

true quantum yields are higher than those determined by absorption changes (apparent).

Gray and co-workers [27] reported similar values for molar absorptivities of *fac*-[Re(CO)$_3$(NN)(*cis*-bpe)]$^+$ complexes, NN = phen, bpy, Me$_2$bpy, Me$_4$phen, although the *trans–cis* photoisomerization quantum yields determined by absorption changes are equal to the values determined by changes in ^{1}H NMR spectra.

In these cases, the absorbance difference, commonly used to determine quantum yields, does give only apparent values. If the contribution of the photoproduct or reactant at the probe wavelength is negligible, the determined value is the true quantum yield, otherwise it gives a value, which is lower than a true quantum yield obtained using an actual concentration of the photoproduct and/or remaining concentration of the reactant. For instance, the absorbance of the free *cis*-L is negligible in the region (300–325 nm) employed to determine quantum yields, Fig. 4, and therefore photoisomerization quantum yields for free *trans*-L determined by absorption and ^{1}H NMR changes, Fig. 5, are similar, Table 3.

Trans to *cis* photoisomerization quantum yields of the free ligands determined by absorption and NMR changes are equal within the experimental error and are in accord with the literature [3–5,8]. Thus, in these cases, the ordinary spectral absorption variation provides the true quantum yields for the photoprocess. Otherwise, ^{1}H NMR spectroscopy proved to be a powerful and efficient technique to determine accurate quantum yields, although some experimental conditions have to be considered. One of them is a good signal to noise ratio requirement at a lower acquisition time, which can be achieved by using high frequency equipments such as a 500 MHz one. Sample concentration has to be adjusted to an absorbance not much higher than 2 at the irradiation wavelength to prevent the inner filter effect. Usually, this is a diluted solution for NMR experiments and consequently a longer acquisition time is needed to obtain a better signal to noise ratio.

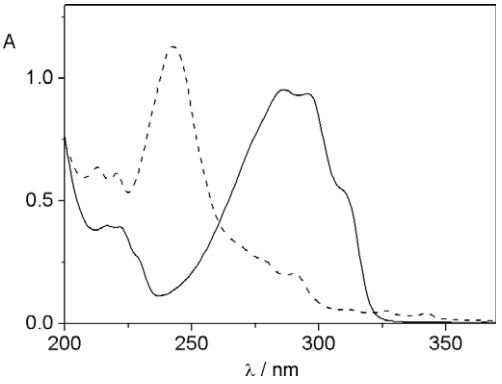

Fig. 4. Absorption spectra of 3.2×10^{-4} mol L^{-1} *trans*-bpe (——) and 84% *cis*-bpe solution (- - -).

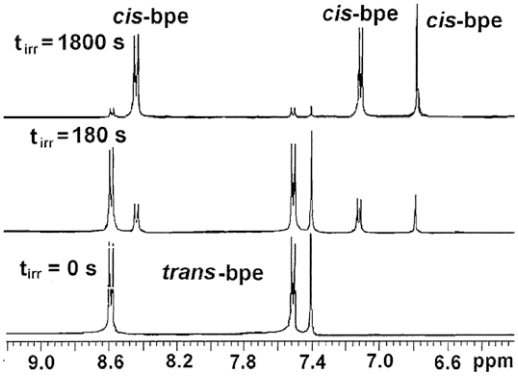

Fig. 5. ^{1}H NMR spectra of *trans*-bpe in CD_3CN upon photolysis at 313 nm. (300 MHz, $T = 298$ K.)

Table 2
Trans–cis photoisomerization quantum yields of *fac*-[Re(CO)$_3$(NN)(*trans*-L)]$^+$ in CD_3CN.

NN	L	313 nm		365 nm		404 nm	
		Φ_{app}[a]	Φ_{true}	Φ_{app}[a]	Φ_{true}	Φ_{app}	Φ_{true}
phen	bpe	0.41 ± 0.02	0.81 ± 0.07	0.39 ± 0.02	0.80 ± 0.07	0.38 ± 0.04	0.77 ± 0.09[b]
	stpy	0.35 ± 0.02	0.59 ± 0.05[b]	0.31 ± 0.02	0.60 ± 0.06	0.29 ± 0.03	0.43 ± 0.02
ph$_2$phen	bpe	0.21 ± 0.02	0.43 ± 0.03	0.17 ± 0.01	0.44 ± 0.02	0.19 ± 0.01	0.43 ± 0.02
	stpy	0.30 ± 0.02	0.60 ± 0.05	0.32 ± 0.05	0.64 ± 0.09	0.20 ± 0.02	0.42 ± 0.03

[a] [19].
[b] Obtained by using molar absorptivities for *cis*-complexes.

Table 3
Trans–cis isomerization quantum yields for uncoordinated *trans*-bpe and *trans*-stpy in CD_3CN solution. (λ_{irr} = 313 nm).

Compound	Φ (UV–Vis)	Φ (^{1}H NMR)
trans-bpe	0.27 ± 0.04 0.25[a]	0.26 ± 0.04
trans-stpy	0.49 ± 0.03 0.46[b]	0.49 ± 0.04

[a] 70% Acetonitrile/30% water [3,4,19].
[b] Acetonitrile $_{irr}$ = 320 nm [8,19].

4. Conclusion

Absorption spectral change is an accessible and readily available technique widely employed to determine quantum yields. When both the photoproduct and the reactant absorb in the same spectral region, e.g. the photoisomerization of *trans*-L in *fac*-[Re(CO)$_3$(NN)(*trans*-L)]$^+$ complexes, the use of this technique itself does not provide true quantum yields. In these cases, the ^{1}H NMR spectroscopy has been successfully employed and proved to be an important tool to determine accurate quantum yields since the proton signals for photoproduct and reactant appear in different regions. As a consequence, quantum yields so determined are the true ones while those determined by variations in absorption spectra are apparent. Besides the true quantum yield determination, the ^{1}H NMR technique, when combined with the absorption spectroscopy, allows the determination of photoproducts molar absorptivities. Then, the determination of true quantum yields can be provided by the use of the faster and low-cost absorption spectrum experiment.

Acknowledgements

The authors are grateful to the Fundação de Amparo à Pesquisa do Estado de São Paulo (FAPESP) and the Conselho Nacional de Desenvolvimento Científico e Tecnológico (CNPq) for the financial support.

References

[1] A.R. Olson, Trans. Faraday Soc. 27 (1931) 69.
[2] D.G. Whitten, M.T. McCall, J. Am. Chem. Soc. 91 (1969) 5097.
[3] D.G. Whitten, Y.J. Lee, J. Am. Chem. Soc. 92 (1970) 415.
[4] Y.J. Lee, D.G. Whitten, L. Pedersen, J. Am. Chem. Soc. 93 (1971) 6330.
[5] G. Bartocci, P. Bortolus, U. Mazzucato, J. Phys. Chem. 77 (1973) 605.
[6] M.S. Wrighton, D.L. Morse, L. Pdungsap, J. Am. Chem. Soc. 97 (1975) 2073.
[7] J. Saltiel, A.S. Waller, D.F. Sears Jr., J. Photochem. Photobiol., A 65 (1992) 29.
[8] H. Görner, H.J. Kuhn, Adv. Photochem. 19 (1995).
[9] D.M. Dattelbaum, M.K. Itokazu, N.Y. Murakami Iha, T.J. Meyer, Phys. Chem. A 107 (2003) 4092.
[10] A.O.T. Patrocínio, N.Y. Murakami, Inorg. Chem. 47 (2008) 10851.
[11] M. Wrighton, D.L. Morse, J. Am. Chem. Soc. 96 (1974) 998.
[12] V.W.W. Yam, V.C.Y. Lau, K.K. Cheung, J. Chem. Soc., Chem. Commun. (1995) 259–261.
[13] V.W.W. Yam, V.C.Y. Lau, L.X. Wu, J. Chem. Soc., Dalton Trans. (1998) 1461–1468.
[14] S.S. Sun, A.J. Lees, J. Am. Chem. Soc. 122 (2000) 8956.
[15] V.W.W. Yam, Y. Yang, J. Zhang, B.W.K. Chu, N. Zhu, Organometallics 20 (2001) 4911.
[16] R. Argazzi, E. Bertolasi, C. Chiorboli, C.A. Bignozzi, M.K. Itokazu, N.Y. Murakami, Inorg. Chem. 40 (2001) 6885.
[17] M.K. Itokazu, A.S. Polo, D.L.A. De Faria, C.A. Bignozzi, N.Y. Murakamiha, Inorg. Chim. Acta 313 (2001) 149.
[18] A.S. Polo, M.K. Itokazu, N.Y. Murakami, J. Photochem. Photobiol., A: Chem. 181 (2006) 73.
[19] A.S. Polo, M.K. Itokazu, K.M. Frin, Coord. Chem. Rev. 250 (2006) 1669.
[20] K.M. Frin, N.Y. Murakami, J. Braz. Chem. Soc. 17 (2006) 1664.
[21] M. Busby, P. Matousek, M. Towrie, A. Vlcek Jr., J. Phys. Chem. A 109 (2005) 3000.
[22] O.S. Wenger, L.M. Henling, M.W. Day, J.R. Winkler, H.B. Gray, Polyhedron 23 (2004) 2955.
[23] C.A. Parker, C.G. Hatchard, J. Phys. Chem. 63 (1959) 22.
[24] N. Murakami Iha, G. Ferraudi, J. Chem. Soc., Dalton Trans. (1994) 2565–2571.
[25] M.K. Itokazu, A.S. Polo, N.Y. Murakami, J. Photochem. Photobiol., A: Chem. 160 (2003) 27.
[26] H.J. Kuhn, S.E. Braslavsky, R. Schmidt, Pure Appl. Chem. 76 (2004) 2105.
[27] O.S. Wenger, L.M. Henling, M.W. Day, J.R. Winkler, H.B. Gray, Inorg. Chem. 43 (2004) 2043.